Check for updates

ORIGINAL RESEARCH

Fully Automated Cardiac Assessment for Diagnostic and Prognostic Stratification Following Myocardial Infarction

Andreas Schuster (iD), MD, PhD, MBA*; Torben Lange (iD), MD*; Sören J. Backhaus, MD; Carolin Strohmeyer, BSc; Patricia C. Boom, BSc; Jonas Matz, BSc; Johannes T. Kowallick, MD; Joachim Lotz, MD; Michael Steinmetz, MD; Shelby Kutty, MD, PhD, MHCM; Boris Bigalke, MD, MBA, LLM; Matthias Gutberlet, MD; Suzanne de Waha-Thiele, MD; Steffen Desch, MD; Gerd Hasenfuß, MD; Holger Thiele, MD; Thomas Stiermaier (iD), MD†; Ingo Eitel (iD), MD†

BACKGROUND: Cardiovascular magnetic resonance imaging is considered the reference methodology for cardiac morphology and function but requires manual postprocessing. Whether novel artificial intelligence–based automated analyses deliver similar information for risk stratification is unknown. Therefore, this study aimed to investigate feasibility and prognostic implications of artificial intelligence–based, commercially available software analyses.

METHODS AND RESULTS: Cardiovascular magnetic resonance data (n=1017 patients) from 2 myocardial infarction multicenter trials were included. Analyses of biventricular parameters including ejection fraction (EF) were manually and automatically assessed using conventional and artificial intelligence–based software. Obtained parameters entered regression analyses for prediction of major adverse cardiac events, defined as death, reinfarction, or congestive heart failure, within 1 year after the acute event. Both manual and uncorrected automated volumetric assessments showed similar impact on outcome in univariate analyses (left ventricular EF, manual: hazard ratio [HR], 0.93 [95% CI 0.91–0.95]; $P<0.001$; automated: HR, 0.94 [95% CI, 0.92–0.96]; $P<0.001$) and multivariable analyses (left ventricular EF, manual: HR, 0.95 [95% CI, 0.92–0.98]; $P=0.001$; automated: HR, 0.95 [95% CI, 0.92–0.98]; $P=0.001$). Manual correction of the automated contours did not lead to improved risk prediction (left ventricular EF, area under the curve: 0.67 automated versus 0.68 automated corrected; $P=0.49$). There was acceptable agreement (left ventricular EF: bias, 2.6%; 95% limits of agreement, −9.1% to 14.2%; intraclass correlation coefficient, 0.88 [95% CI, 0.77–0.93]) of manual and automated volumetric assessments.

CONCLUSIONS: User-independent volumetric analyses performed by fully automated software are feasible, and results are equally predictive of major adverse cardiac events compared with conventional analyses in patients following myocardial infarction.

REGISTRATION: URL: https://www.clinicaltrials.gov; Unique identifiers: NCT00712101 and NCT01612312.

Key Words: artificial intelligence ■ automated postprocessing ■ cardiac magnetic resonance imaging ■ deep learning software ■ risk stratification

Because cardiovascular disease remains the major cause of premature death, risk stratification plays a fundamental role in clinical practice.[1] Cardiovascular magnetic resonance (CMR) has emerged as reference standard for left ventricular (LV) and right ventricular (RV) cardiac function and

JAHA is available at: www.ahajournals.org/journal/jaha

CLINICAL PERSPECTIVE

What Is New?

- In this study, fully automated myocardial segmentation of cardiac magnetic resonance images provided risk prediction of hard clinical events similar to that of manual analyses in a large cohort of patients following myocardial infarction.

What Are the Clinical Implications?

- Fully automated myocardial segmentation has great potential for a more time-efficient post-processing with automated delivery of prognostically relevant cardiac magnetic resonance parameters, which may allow broad adoption of risk stratification without impeding diagnostic workflow in clinical practice.

Nonstandard Abbreviations and Acronyms

AI	artificial intelligence
AMI	acute myocardial infarction
CMR	cardiovascular magnetic resonance
IS	infarct size
LOA	limits of agreement
LVEF	left ventricular ejection fraction
MACE	major adverse cardiac events
MVO	microvascular obstruction
NSTEMI	non–ST-segment–elevation myocardial infarction
SAX	short axis
STEMI	ST-segment–elevation myocardial infarction

infarct size (IS) quantification following acute myocardial infarction (AMI).[2] LV and RV end-diastolic and end-systolic contours are usually manually delineated to derive myocardial mass and volumetric data. Myocardial damage or IS quantification additionally requires manual or semiautomated delineation of areas with gadolinium uptake on late gadolinium enhanced (LGE) images. Because this process is time consuming, technical developments have been directed at automation, less user interaction, and time saving. Novel artificial intelligence (AI)–based[3] deep learning algorithms were recently introduced and may provide accurate, fully automated image analyses using convolutional neural networks.[4] The accuracy of this machine-learning approach has been shown for scan-rescan examinations and different selected cardiac diseases.[5,6] However, the comparability to manual analysis and the feasibility and diagnostic utility for risk prediction following AMI have not yet been demonstrated in a large patient data set following AMI. Therefore, the aim of this study was to perform fully automated biventricular volumetric and LV IS quantification in comparison to manual analyses using commercially available software and to study their relative prognostic implications in a large multicenter cohort of patients after AMI.

METHODS

Study Population

The data that support the findings of this study are available from the corresponding author on reasonable request. The study population consisted of patients initially recruited for the trials AIDA STEMI (Abciximab i.v. versus i.c. in ST-elevation Myocardial Infarction; ClinicalTrials.gov ID: NCT00712101)[7] and TATORT-NSTEMI (Thrombus Aspiration in Thrombus Containing Culprit Lesions in Non-ST-Elevation Myocardial Infarction; ClinicalTrials.gov ID: NCT01612312).[8]

The AIDA STEMI trial encompassed 2065 patients with ST-segment–elevation myocardial infarction (STEMI). After assigning the group to either intracoronary (n=1032) or intravenous (n=1033) abciximab application, a drug bolus (0.25 mg/kg body weight) was given during percutaneous coronary intervention, followed by continuous intravenous infusion for 12 hours (0.125 µg/kg per minute, maximum of 10 µg/min). Subsequently, CMR imaging was performed at 8 different sites in 795 patients.

The TATORT-NSTEMI trial enrolled 440 patients with non-STEMI (NSTEMI) and randomized them to either treatment by percutaneous coronary intervention and aspiration thrombectomy (n=221) or percutaneous coronary intervention without thrombus aspiration (n=219). The study end points included microvascular injury as defined by CMR imaging. CMR imaging was performed within 10 days after symptom onset in both trials. There was no difference between intervention and control arms in both trials, respectively. All patients gave written informed consent before participation. Both studies were approved by the respective ethics committees of the lead institution at the University of Leipzig and all participating study sites and complied with the principles of the Helsinki Declaration.

Clinical End Points

The occurrence of major adverse cardiac events (MACE) was defined as the primary clinical end point of the study, which included all-cause mortality, reinfarction, and congestive heart failure. Only 1 MACE could be attributed to each patient. In case of the occurrence of ≥2 adverse events within 1 patient, an order of

priority was set (in descending order: death, reinfarction, congestive heart failure).

CMR Imaging

CMR imaging was performed using standardized scanning protocols on 1.5- or 3.0-T scanners at the different study sites. The scan protocol included long- and short-axis (SAX) steady-state free precession images (repetition time, 3.2 ms; echo time, 1.2 ms; flip angle, 60°; slice thickness, 8 mm), T2-weighted triple short-τ inversion recovery images (repetition time, 2 RR intervals; echo time, 80 ms; flip angle, 90°) and T1-weighted LGE imaging (repetition time, 2.8 ms; echo time, 1.1 ms; flip angle, 15°; slice thickness, 8 mm, with individually adjusted inversion times typically between 200 and 300 ms). LGE imaging was acquired 10 to 20 minutes after injection of a gadolinium-based contrast agent bolus (0.15 mmol/kg).[7,8] Participants with typical contraindications for CMR examination were excluded.[8]

Volumetric Analyses

All patients with SAX stacks covering base to apex with all slices of equal cardiac phases were included in the final analysis. Patients without coverage of the entire LV or uneven number of cardiac phases within respective slices were excluded. Manual volumetric analyses were performed based on SAX steady-state free precession–Cine images by an experienced investigator using commercially available postprocessing software (cvi42; Circle Cardiovascular Imaging; Figure 1).

Fully automated volumetric analyses were performed by applying commercially available AI software (suiteHEART, v4.0.6; Neosoft).

Analyzed volumetric parameters included LV mass, LV ejection fraction (LVEF), RV ejection fraction,
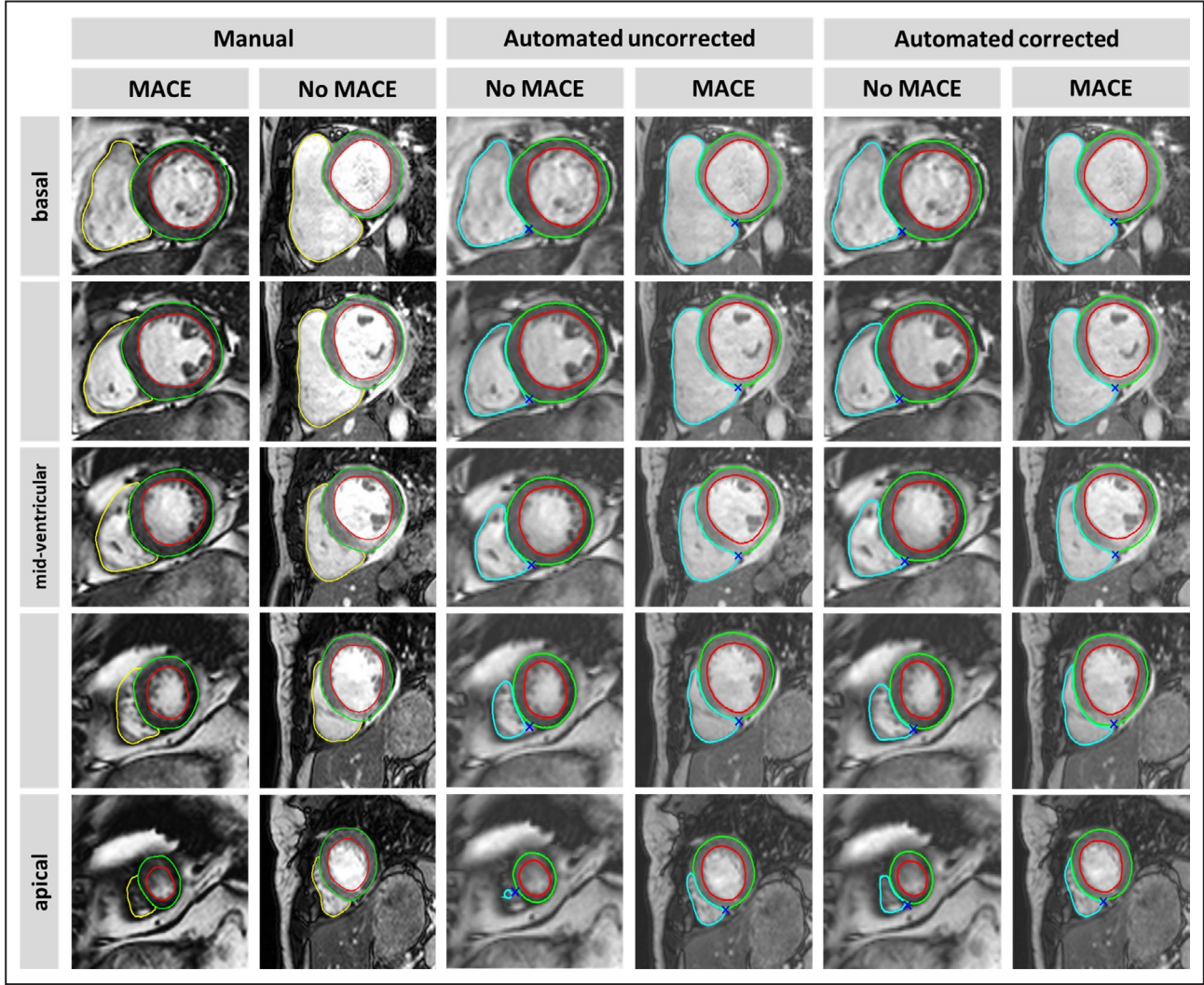

Figure 1. Automated, automated corrected, and manual biventricular volumetric analyses.
Overview of a tracked short-axis stack from base to apex of 1 patient with and without MACE each using different analysis software types. MACE indicates major adverse cardiac events.

end-diastolic volume (EDV), end-systolic volume (ESV), and stroke volume. For manual analyses, LV endo- and epicardial borders and RV endocardial borders were delineated at end-systole and end-diastole. In accordance with current recommendations, the papillary muscles were excluded from the myocardium using both software types.[9]

For automated analysis, the software algorithm was run overnight with no further pre- or postprocessing user interactions performed. In a second step, all automatically traced borders were evaluated visually and corrected if the delineation of the ventricular borders was not in accordance with clinical practice recommendations.[9] The extent of corrections was documented, with a major tracking failure defined as false contouring on extracardiac structures or complete deviations of the endocardial or epicardial curvature. In addition, time needed for visual evaluation and, if necessary, for correction of the contours was documented. Image quality was evaluated by using quality criteria defined by Klinke et al.[10] Depending on the presence and extent of artifacts (eg, wraparound, respiratory or cardiac ghost, image blurring, metal and shimming artifacts), a graduation based on a score 0 to 3 was made. For this purpose, 1 point was given if more than one-third of the ventricular endocardial border on a single SAX slice was affected by an artefact at end-systole or end-diastole. If 2 or ≥3 slices were impeded by an artifact, 2 or 3 points were given, respectively.

IS Analyses

Manual IS quantification was performed on T1-weighted SAX LGE images from base to apex according to current guidelines using dedicated software (QMass, v3.1.16.0; Medis Medical Imaging Systems).[9] In addition to IS microvascular obstruction (MVO) was analyzed. For automated analyses, the software algorithm was applied overnight (suiteHEART, v4.0.7; Neosoft). Based on a full-width half-maximum approach, which has been shown to be most comparable with manual LGE assessment to define thresholds for enhanced and nonenhanced myocardium,[11] the algorithm automatically delineated LV myocardium and identified enhanced areas. Hypointense infarct cores had to be manually included if present. In a second step, the automated enhancement detection was corrected manually in case of erroneous contour delineation or identification of artifacts or blood pool as LGE and named automated corrected IS (Figure 2).

Statistical Analysis

Statistical analyses were performed using SPSS Statistics v25 (IBM Corp) and Microsoft Excel, Microsoft Office 2019 (Microsoft). Categorical variables are presented as absolute numbers and percentages. Continuous parameters were tested for normal distribution using the Shapiro–Wilk test and reported as median and interquartile range. The Mann–Whitney U test was performed to compare continuous parameters, and the χ^2 test was applied for categorical values. Dependent variables were tested using the Wilcoxon signed rank test. Statistical calculations were made both for the overall collective and for predefined subgroups of patients with STEMI or NSTEMI. Correlations were assessed using the Spearman rank correlation coefficient. For assessing concurrence of manual and automated analyses, the following calculations were made: according to established Bland-Altman analysis, the difference between measurements of both approaches was defined as bias estimated by the mean difference. In addition, the 95% limits of agreement calculated by the mean difference ±1.96 SD of the mean difference were reported. Furthermore, corresponding Bland-Altman plots were generated.[12] Intraclass correlation coefficients (ICC) using a model of absolute agreement considered as excellent if ICC was >0.74, good between 0.60 and 0.74, fair at 0.40 to 0.59, and poor at <0.40.[13,14] The coefficient of variation, defined as the standard deviation of the differences divided by the mean, was implemented.[15] The Kaplan–Meier method was applied for clinical end point assessment, with the cohort dichotomized at LVEF 35% as a clinically relevant cutoff value in each manual and automated group. To identify independent predictors of MACE, univariate and multivariable Cox regression calculations providing hazard ratios (HR) with corresponding 95% CIs were performed. Only parameters with $P<0.05$ on univariate analyses were included in further multivariable modeling. Although model 1 included LVEF, a second statistical model was implemented to identify associations of manual and automated IS with MACE. Given high correlation, and to enable a focused calculation for prognostic implementation of IS, LVEF was not included in model 2.

To assess the additional predictive value of automatically generated volumetric parameters, receiver operator characteristics were implemented. For both methods, area under the curve (AUC) values for MACE prediction were calculated and compared using the nonparametric approach by DeLong et al.[16] All P values provided are 2-sided, and $P<0.05$ was considered statistically significant.

RESULTS

Study Population

For overall volumetric analyses, 1017 patient data sets were available. Among this cohort, 795 patients had
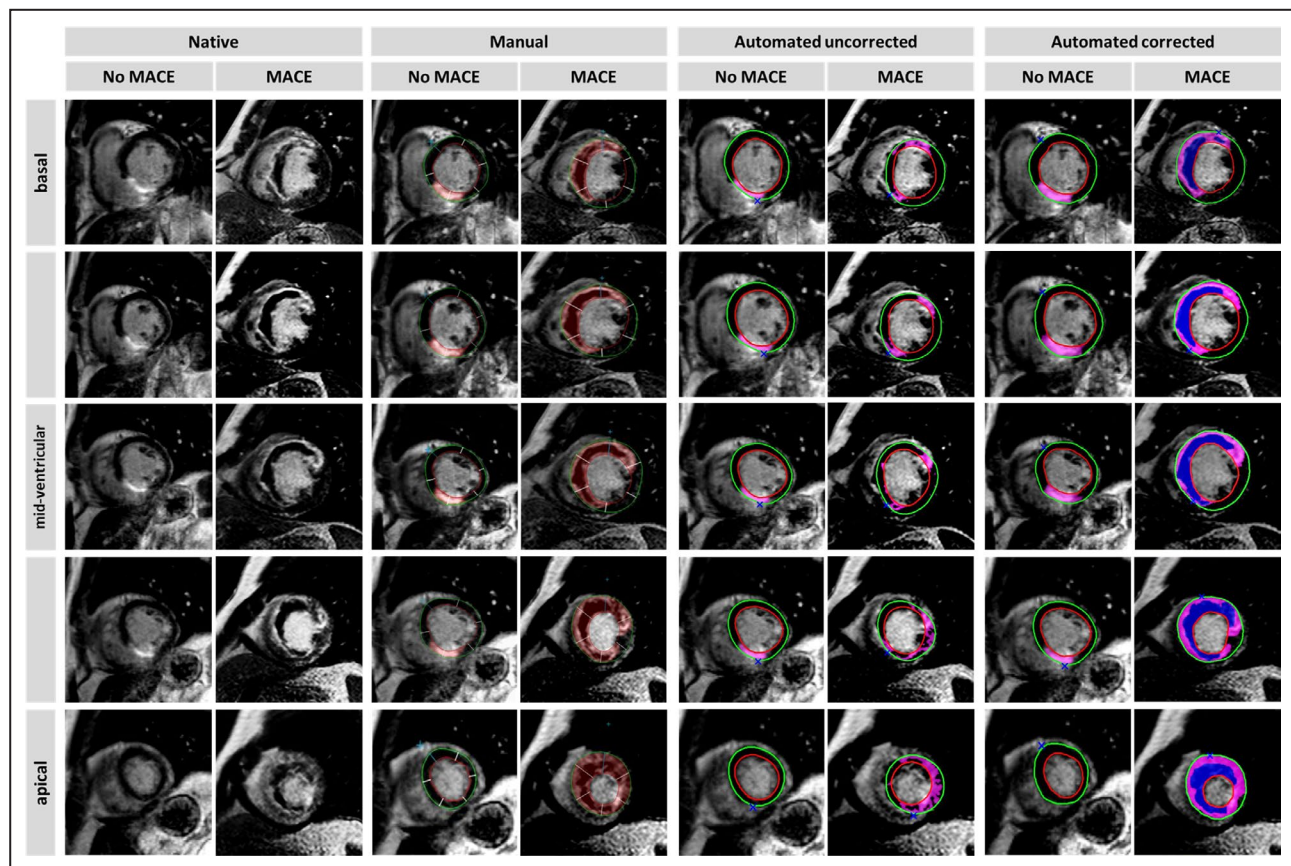
Figure 2.   Automated, automated corrected, and manual quantification of enhancement detection.
Overview of IS detection in short-axis orientation from base to apex of 1 patient with and without MACE. IS indicates infarct size; MACE indicates major adverse cardiac events.

STEMI and 292 had NSTEMI. Overall, 913 patients had presence of LGE (668 STEMI and 245 NSTEMI) and entered manual and automated LGE quantification (Figure 3). A detailed overview of the baseline characteristics is presented in Table 1. All patients underwent CMR scanning in a median of 3 days (interquartile range, 2–4 days) after the acute event. Cardiovascular risk factors were more frequent in patients with MACE during follow-up (hypertension, P=0.01; diabetes mellitus, P=0.02). Moreover, Killip class on admission and the number of diseased vessels were significantly higher in patients with MACE (P<0.001 and P=0.004, respectively). Neither the affected artery nor the TIMI (Thrombolysis in Myocardial Infarction) flow before or after the coronary intervention demonstrated a significant difference between patients with and without MACE.

Automatically and Manually Derived Volumetric Parameters

Automated segmentation was feasible in all patients, and no major tracking failure was documented.

Volumetric analyses revealed considerable differences in absolute numbers between manual and automatic biventricular segmentation that are reported in Table 2. Both LV and RV volumes were estimated higher by automatic software analysis, whereas LV mass and biventricular ejection fraction were computed lower than manual evaluation (P<0.001 for all). Bias with 95% limits of agreement (LOA), ICC, and coefficient of variation displaying agreement of automated and manual analyses for the overall collective are displayed in Table 3. Corresponding Bland-Altmann plots were generated and are presented in Figure 4. Agreement of both methods was better for LV parameters than for RV parameters. For all LV parameters, agreement was acceptable and best for LVEF (bias, 2.6%; 95% LOA, −9.1% to 14.2%; ICC, 0.89) followed by LV ESV (bias, −15.6 mL; 95% LOA, −46.0 to 15.6 mL; ICC, 0.87) and LV EDV (bias, −22.4 mL; 95% LOA, −59.7 to 14.9 mL; ICC, 0.86). Regarding RV volumetric analysis, agreement was best for ESV (bias, −13.4 mL/m²; 95% LOA, −42.9 to 15.9 mL; ICC, 0.80) and EDV (bias, −23.2 mL; 95% LOA, −64.8 to 18.1 mL; ICC, 0.79), followed by
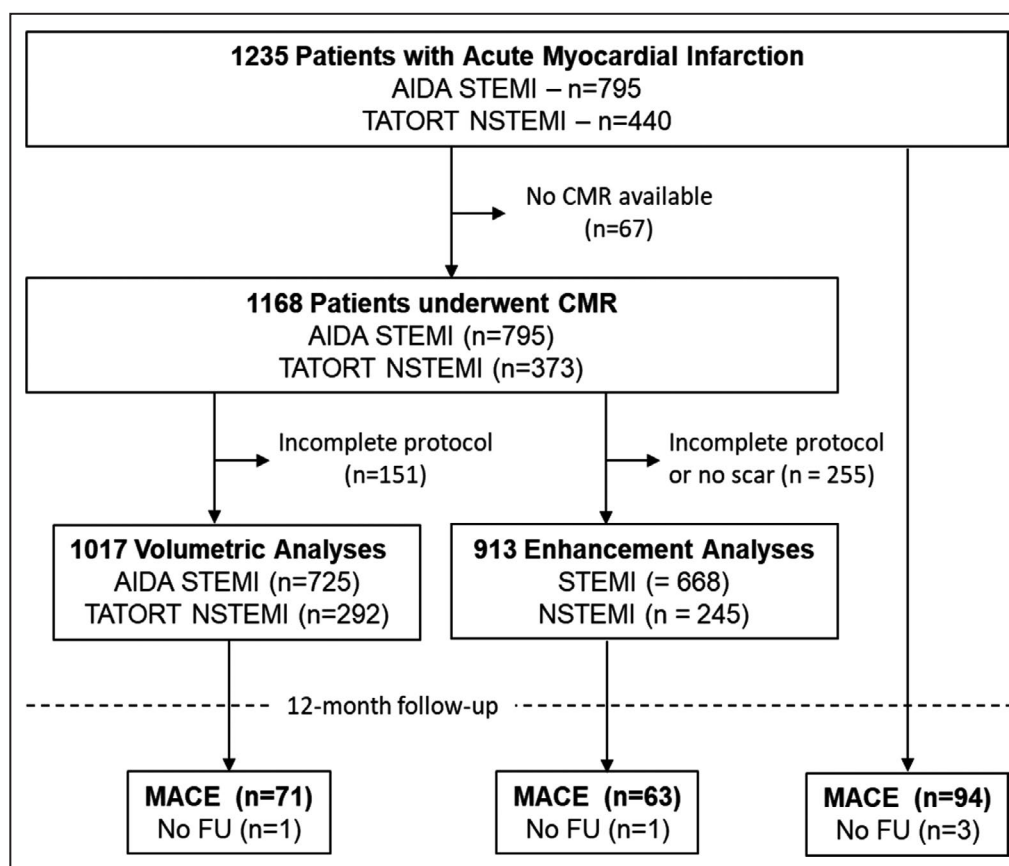
Figure 3.   Study flow chart.
AIDA STEMI indicates Abciximab i.v. versus i.c. in ST-elevation Myocardial Infarction; CMR, cardiac magnetic resonance; FU, follow-up; MACE indicates major adverse cardiac events; NSTEMI, non–ST-segment–elevation myocardial infarction; STEMI, ST-segment–elevation myocardial infarction; and TATORT NSTEMI, Thrombus Aspiration in Thrombus Containing Culprit Lesions in Non-ST-Elevation Myocardial Infarction.

ejection fraction (bias, 3.0%; 95% LOA, −40.4% to 20.8%; ICC, 0.71) and stroke volume (bias, −9.8 mL; 95% LOA, −13.9 to 19.9 mL; ICC, 0.73).

Image quality was good in the majority of patients (906 patients with score 0 [89%], 14 patients with score 1 [1.4%], 22 patients with score 2 [2.2%], and 75 patients with score 3 [7.4%]). Agreement of the parameters was better in data sets with high imaging quality (image quality, 0–1 point), lowering the LVEF's mean difference from 2.6% (95% LOA, −9.1% to 14.2%) in the overall collective to 0.8% (LOA, −7.48% to 9.06%).

The mean postprocessing duration of core laboratory masked conventional volumetric analysis by an experienced investigator took about 12 minutes. The mean time for contour computation using automated software took about 40 seconds. Reviewing the automated contours took about 1 minute, followed by an additional mean correction time of 1.2 minutes if needed. In total, 644 patients (63%) underwent mostly minor contour optimizations, which were more often required for the LV than in RV mostly because of infarct

areas reducing the contrast between blood pool and myocardium. Among these 644 patients, 28.7% received both LV and RV corrections, 47.1% underwent only LV corrections, and 24.2% underwent only RV corrections. The optimizations led to a numerically better agreement with manual analyses for all parameters, with LVEF retaining highest agreement (bias, 0.96; 95% LOA, −7.4% to 9.3%; ICC, 0.94) (Table 4).

Automatically and Manually Derived IS

Comparison of automated uncorrected and manually derived IS quantification revealed considerable differences in absolute numbers ($P<0.001$) (Table 2). Agreement of automated and manual enhancement quantification was acceptable (LV mass: bias, −7.98%, 95% LOA, −22.9 to 6.9%; ICC, 0.75) and was further improved by correcting the automatically marked infarct area (LV mass: bias, −0.2%; 95% LOA, −6.8 to 6.3%; ICC, 0.98) with no remaining difference compared with the manual approach ($P=0.07$) (Figure S1).

Table 1.   **Baseline Characteristics**

Variables	All Patients (n=1017)	STEMI (n=725)	NSTEMI (n=292)	MACE (n=71)	No MACE (n=945)	P Value
Age, y	64 (53–72)	62 (51–71)	68 (56–74)	72 (61–77)	63 (52–72)	<0.001*
Sex (male)	763/1017 (75.0)	547/725 (75.4)	216/292 (74.0)	45/71 (63.4)	718/945 (76.0)	0.018*
Cardiovascular risk factors						
Active smoking	404/942 (42.9)	303/665 (45.6)	101/277 (36.5)	17/64 (27.1)	387/877 (44.1)	0.006*
Hypertension	721/1016 (71.0)	496/724 (68.5)	225/292 (77.1)	60/71 (84.5)	660/944 (69.9)	0.009*
Hyperlipoproteinemia	379/1011 (37.5)	274/719 (38.1)	105/292 (36.0)	24/71 (33.8)	355/939 (37.8)	0.502
Diabetes mellitus	233/1016 (22.9)	149/724 (20.6)	84/292 (28.8)	24/71 (33.8)	208/944 (22.0)	0.023*
Body mass index, kg/m^2	27.4 (25–30.3)	27.3 (24.9–30.2)	27.7 (25–30.5)	27.3 (25.4–31.1)	27.4 (25.0–30.2)	0.569
Previous myocardial infarction	72/1016 (7.1)	43/725 (5.9)	29/292 (9.9)	5/71 (7.0)	67/944 (7.1)	0.986
Previous PCI	84/1017 (8.3)	59/725 (8.1)	25/292 (8.6)	4/71 (5.6)	80/945 (8.3)	0.911
Previous CABG	19/1017 (1.9)	10/725 (1.4)	9/292 (3.1)	2/71 (2.9)	17/945 (1.8)	0.542
ST-segment elevation	725/1017 (71.3)	725/725 (100.0)	0/292 (0.0)	51/71 (71.8)	674/945 (71.3)	0.404
Systolic blood pressure, mm Hg	133 (118–150)	130 (117–148)	140 (120–159)	130 (110–144)	134 (120–150)	0.042*
Diastolic blood pressure, mm Hg	80 (70–89)	80 (70–88)	80 (70–90)	77 (64–84)	80 (70–90)	0.031*
Heart rate, beats/min	76 (67–86)	76 (67–87)	76 (66–85)	80 (70–94)	76 (66–85)	0.002*
Time symptoms to balloon,* min	180 (110–327)	180 (110–327)		191 (116–376)	180 (110–315)	0.423
Door-to-balloon time,* min	30 (22–42)	30 (22–42)		28 (22–40)	30 (22–42)	0.439
Killip class on admission						<0.001*
1	908/1017 (89.3)	636/725 (87.7)	272/292 (93.2)	49/71 (69.0)	858/945 (90.8)	
2	75/1017 (7.4)	56/725 (7.7)	19/272 (6.5)	14/71 (19.7)	61/945 (6.5)	
3	20/1017 (2.0)	19/725 (2.6)	1/292 (0.3)	4/71 (5.6)	16/945 (1.7)	
4	14/1017 (1.4)	14/725 (1.9)	0/292 (0.0)	4/71 (5.6)	10/945 (1.1)	
Diseased vessels						0.004*
1	511/1016 (50.2)	383/726 (52.8)	128/292 (43.8)	26/71 (36.6)	484/945 (51.2)	
2	306/1016 (30.1)	203/726 (28.0)	103/292 (35.2)	22/71 (31.0)	284/945 (30.1)	
3	200/1016 (19.7)	139/726 (19.2)	61/292 (20.9)	23/71 (32.4)	177/945 (18.7)	
Affected artery						0.233
Left anterior descending	432/1017 (42.5)	326/725 (45.0)	106/292 (36.3)	39/71 (54.9)	393/945 (41.6)	
Left circumflex	195/1017 (19.2)	80/725 (11.0)	115/292 (39.4)	12/71 (16.9)	182/945 (19.3)	
Left main	5/1017 (0.5)	5/725 (0.7)	0/292 (0.0)	0/71 (0.0)	5/945 (0.5)	
Right coronary artery	379/1017 (37.3)	312/725 (43.0)	67/292 (22.9)	19/71 (26.8)	360/945 (38.1)	
Bypass graft	6/1017 (0.6)	2/725 (0.3)	4/292 (1.4)	1/71 (1.4)	5/945 (0.5)	
TIMI flow grade before PCI						0.217
0	512/1017 (50.3)	400/725 (55.2)	112/292 (38.4)	42/71 (57.2)	470/945 (49.7)	
1	108/1017 (10.6)	91/725 (12.6)	17/292 (5.8)	5/71 (7.0)	103/945 (10.9)	
2	210/1017 (20.6)	123/725 (17.0)	87/292 (29.8)	12/71 (16.9)	197/945 (20.8)	
3	187/1017 (18.4)	111/725 (15.3)	76/292 (26.0)	12/71 (16.9)	175/945 (18.5)	
Stent implanted	1002/1017 (98)	713/725 (98.2)	285/292 (97.6)	70/71 (98.6)	926/945 (98)	0.525
TIMI flow grade after PCI						0.173
0	18/1017 (1.8)	12/725 (1.7)	6/292 (2.1)	1/71 (1.4)	17/944 (1.8)	
1	22/1017 (2.2)	19/725 (2.6)	3/292 (1.0)	3/71 (4.2)	19/944 (2.0)	
2	80/1017 (7.9)	56/725 (7.7)	24/292 (8.2)	8/71 (11.3)	72/944 (7.6)	
3	897/1017 (88.2)	638/725 (88.0)	259/292 (88.7)	59/71 (83.1)	837/944 (88.6)	
Medication						
Glycoprotein IIb/IIIa inhibitor	744/1022 (72.8)	725/725 (100.0)	274/292 (93.9)	53/71 (74.6)	690/945 (73.0)	0.765
Aspirin	1016/1017 (99.9)	725/725 (100.0)	291/292 (99.7)	71/71 (100.0)	943/945 (99.9)	0.784
Clopidogrel/prasugrel/ticagrelor	1017/1017 (100.0)	726/726 (100.0)	292/292 (100.0)	71/71 (100.0)	944/944 (100.0)	

(*Continued*)

Table 1. Continued

Variables	All Patients (n=1017)	STEMI (n=725)	NSTEMI (n=292)	MACE (n=71)	No MACE (n=945)	P Value
Betablocker	973/1015 (95.9)	692/723 (95.7)	281/292 (96.2)	69/71 (97.2)	903/943 (95.8)	0.561
ACEI/ARB antagonist	937/1015 (92.3)	689/723 (95.3)	248/292 (84.9)	67/71 (94.4)	870/943 (92.3)	0.518
Aldosterone antagonist	134/1015 (13.2)	85//723 ((11.8)	50/292 (16.9)	23/71 (32.4)	111/943 (11.8)	<0.001*
Statin	976/1015 (96.2)	692/723 (95.7)	284/292 (97.3)	68/71 (95.8)	907/943 (96.2)	0.863
Time to MRI, d	3 (2–4)	3 (2–4)	3 (2–4)	3 (2–4)	3 (2–4)	0.036*

Data are presented as n/N (%) or median (interquartile range). For comparison of patients with MACE and no MACE, P values were calculated. One patient was lost to follow-up regarding MACE. ACEI indicates angiotensin-converting enzyme inhibitor; CABG, coronary artery bypass grafting; MACE, major adverse cardiac event; MRI, magnetic resonance imaging; NSTEMI, non–ST-segment–elevation myocardial infarction; PCI, percutaneous coronary intervention; STEMI, ST-segment–elevation myocardial infarction; and TIMI, Thrombolysis in Myocardial Infarction.

*Indicates a statistically significant difference. Mann–Whitney U test was used for testing continuous variables. Categorical variables were tested using the χ^2 test. One patient of the overall collective was lost to follow-up and thus was not considered in MACE analysis.

Manual enhancement analysis took about 11 minutes by an experienced investigator. A review of the automatically traced and marked LGE images took <1 minute per patient. Manual editing of the automated IS quantification took an additional 1 minute and 59 seconds on average. Overall, 169 cases required minimal corrections of endo- or epicardial contours. In almost all patients (896/913), adjustments of the actual enhancement area was required (mean erased area, 7.91%).

Prognostic Value of Automated and Manual Segmentation

Follow-up data revealed MACE in 71 patients within 1 year after the index event (death, n=30; reinfarction, n=21; heart failure, n=20). In the statistical Cox regression model including LVEF, univariate analyses showed significant associations of cardiovascular risk factors and clinical status with MACE (age, P<0.001; sex, P=0.02; hypertension, P=0.01; diabetes mellitus, P=0.02; Killip class on admission, P<0.001). Both manual and automated LVEFs were associated with the occurrence of MACE during follow-up (manual: HR, 0.93 [95% CI, 0.91–0.95]; automated: HR, 0.94 [95% CI, 0.92–0.96]; P<0.001 for both) (Table 5). If divided into STEMI and NSTEMI cohorts, similar results were observed (manual, STEMI: HR, 0.93 [95% CI, 0.91–0.96]; P≤0.001; NSTEMI: HR, 0.93 [95% CI, 0.9–0.97]; P=0.001; automated, STEMI: HR, 0.94 [95% CI, 0.92–0.97]; P<0.001; NSTEMI: HR, 0.93 [95% CI, 0.89–0.97]; P=0.001). Multivariable regression

Table 2. Biventricular Volumes and LV IS Characteristics

Parameter	Study Population		
Sex (female/male)	255/767		
Age, y	64 (53–72)		
Body surface area, m²	1.95 (1.82–2.08)		

	Automated	Manual	P Value
LV mass, g	114 (97.0–132.0)	129.3 (108.5–153.2)	<0.001
LV mass, g/m²	57.8 (51.4–65.5)	66.4 (57.4–76.0)	<0.001
LV EDV, mL/m²	87.5 (75.6–100.5)	73.3 (62.07–85.3)	<0.001
LV ESV, mL/m²	45.5 (36.1–56.6)	35.6 (27.7–45.7)	<0.001
LV SV, mL/m²	40.6 (34.4–46.4)	36.1 (30.7–42.0)	<0.001
LVEF (%)	47.0 (40.0–53.0)	50.3 (43.4–57.5)	<0.001
RV EDV, mL/m²	75.3 (63.3–87.5)	60.6 (51.1–71.3)	<0.001
RV ESV, mL/m²	32.2 (25.8–40.2)	23.2 (17.4–31.3)	<0.001
RV SV, mL/m²	42.4 (35.7–48.7)	36.31 (30.76–42.28)	<0.001
RVEF (%)	57.0 (51.0–62.0)	60.7 (53.9–67.4)	<0.001
Infarct size (% LV mass)*	24.8 (17.8–32.1)	15.8 (8.3–23.5)	<0.001

Continuous variables were compared using Wilcoxon signed rank test and presented as median (interquartile range). EDV indicates end-diastolic volume; ESV, end-systolic volume; IS, infarct size; LV, left ventricular; LVEF, left ventricular ejection fraction; RV, right ventricular; RVEF, right ventricular ejection fraction; and SV, stroke volume.

*In 913 patients with IS on late gadolinium enhancement images.

Table 3. Agreement Between Manual and Automated Uncorrected Analyses

Parameter	Bias	95% LOA	ICC (95% CI)	CoV (%)
LV mass	14.15	−20.4 to 48.7	0.84 (0.35–0.93)	14.2
LV EDV	−22.36	−59.7 to 14.9	0.86 (0.09–0.96)	11.9
LV ESV	−15.58	−46.0 to 15.6	0.88 (0.08–0.96)	18.3
LV SV	−6.78	−32.4 to −6.8	0.82 (0.63–0.90)	17.4
LVEF	2.57	−9.1 to 14.2	0.88 (0.77–0.93)	12.3
RV EDV	−23.21	−64.8 to 18.1	0.79 (0.13–0.93)	15.6
RV ESV	−13.4	−42.9 to 15.9	0.80 (0.10–0.92)	25.7
RVEF	2.97	−40.4 to 20.8	0.70 (0.56–0.76)	14.7
RV SV	−9.8	−13.9 to 19.9	0.73 (0.37–0.86)	20.2
Infarct size	−7.98	−22.9 to 6.9	0.75 (0.07–0.89)	36.0

CoV indicates coefficient of variation; EDV, end-diastolic volume; ESV, end-systolic volume; ICC, intraclass correlation coefficient; LOA, limits of agreement; LV, left ventricular; LVEF, left ventricular ejection fraction; RV, right ventricular; RVEF, right ventricular ejection fraction; and SV, stroke volume.

analysis was established containing either manual or automated LVEF due to high correlation between these parameters. Including only univariate significant parameters into multivariable analyses, both manual and automated LVEF remained significantly associated with MACE (manual: HR, 0.95 [95% CI, 0.93–0.98]; P=0.001; automated: HR, 0.96 [95% CI, 0.93–0.99]; P=0.002). In either model, age and Killip class were also independently significant parameters (age: P=0.04 for both manual and automated; Killip class: P=0.03 for manual and P=0.02 for automated).

In a second statistical model including all patients with analyzable IS, univariate Cox regression analyses showed significant associations of both manual and automated uncorrected enhancement assessment with outcome (manual: HR, 1.04 [95% CI, 1.02–1.06]; P<0.001; automated uncorrected: HR, 1.05 [95% CI, 1.02–1.07]; P<0.001). Moreover, manually and automatically derived IS were significantly associated with MACE after correction for univariate significant age, cardiovascular risk factors, Killip class, and number of diseased vessels on multivariable regression analyses (Table 6).

Dichotomization of the patient cohort by the LVEF cutoff of 35% in both the automated and manual groups allowed adequate risk stratification based on clinical end points and Kaplan–Meier analyses (Figure 5). There was no statistically significant difference between manual and automated LVEF on AUC comparison (LVEF, AUC: 0.69 versus 0.67; P=0.11) Furthermore, manual adjustments of the automated contours did not provide further improved risk prediction (LVEF automated, AUC: 0.67 versus 0.68 corrected, P=0.49) or lead to a significant change in uni- or multivariable regression results.

DISCUSSION

This study is the first to investigate the performance of a commercially available novel AI-based automated volume and IS quantification tool and to define its predictive value for further clinical risk stratification in
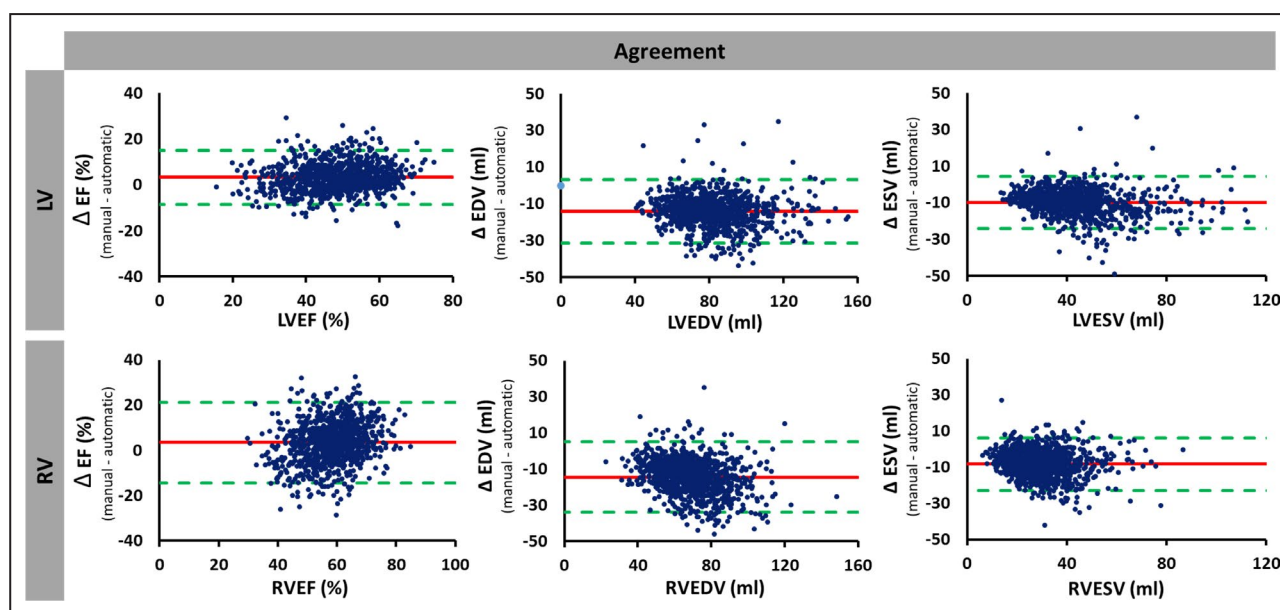
Figure 4. Bland-Altmann plots for agreement of manual and automated biventricular volumes.
Agreement of ventricular parameters derived by automatic and manual analyses. Bland-Altman plots (manual–automatic) are shown. EDV, end-diastolic volume; EF, ejection fraction; ESV, end-systolic volume; LV, left ventricular; and RV, right ventricular.

Table 4. Agreement Between Manual and Automated Corrected Analyses

Parameter	Bias	95% LOA	ICC (95% CI)	CoV (%)
LV mass	10.79	−30.3 to 51.9	0.83 (0.67–0.90)	16.6
LV EDV	−20.05	−54.6 to 14.5	0.88 (0.0–0.96)	11.1
LV ESV	−12.03	−47.1 to 23.1	0.88 (0.62–0.95)	21.7
LV SV	−8.38	−30.9 to 14.1	0.84 (0.44–0.93)	15.1
LVEF	0.96	−7.4 to 9.3	0.94 (0.93–0.95)	8.6
RV EDV	−21.68	−59.2 to 15.8	0.81 (0.0–0.94)	14.3
RV ESV	−13.37	−40.7 to 14.0	0.81 (0.05–0.93)	24.2
RVEF	−8.4	−31.4 to 14.6	0.74 (0.58–0.82)	9.3
RV SV	−8.22	−34.9 to 18.4	0.79 (0.0–0.89)	17.8
Infarct size	−0.2	−6.8 to 6.3	0.98 (0.97–0.98)	19.4

CoV indicates coefficient of variation; EDV, end-diastolic volume; ESV, end-systolic volume; ICC, intraclass correlation coefficient; LOA, limits of agreement; LV, left ventricular; LVEF, left ventricular ejection fraction; RV, right ventricular; RVEF, right ventricular ejection fraction; and SV, stroke volume.

a large cohort of patients following AMI. Several notable findings should be considered. First, automatically derived LVEF based on uncorrected contours has similar significant association with MACE occurrence compared with manually derived LVEF; therefore, it can be equally used for risk prediction. Second, adjustments of the initial volumetric contours aiming for an optimal visual delineation did not lead to improved risk stratification and, consequently, are not mandatory for this purpose. Third, even though IS quantification derived from the automated software enables risk prediction similar to manual IS quantification, user

interaction including confirmation of MVO areas is still required. Therefore, at present, this tool does not yet readily allow fully automated user-independent clinical use. Fourth, applying automated software in the postprocessing routine yields substantial time savings compared with a conventional manual method and can be performed instantly while scanning. Taken together, automated user-independent volumetric analyses represent a software-based tool to facilitate the clinical postprocessing routine, potentially allowing for more efficient risk prediction and management of patients following AMI.

Deep learning algorithms are of increasing importance for the development of cardiovascular medicine. With the help of convolutional neuronal networks, these algorithms mimic human cognition processes, which are fundamental for automated image recognition and analyses.[17] Basically, a wide range of potential advantages exist using an assisting automated software tool in the clinical imaging routine. Analyses are objective with minimal observer influence, the application improves the work efficiency, and thus might reduce costs.[4] Consequently, practical implementations of AI in different cardiac diagnostic modalities have already been made, and results are promising. With the help of AI software, Betancur et al[18] demonstrated higher sensitivity in diagnosing coronary obstructive disease based on automated myocardial perfusion analyses. AI-based image assessment further enables determination of novel noninvasive imaging biomarkers by profiling coronary arteries in coronary computed

Table 5. Univariate and Multivariable Cox Regression Analysis Including LVEF for Prediction of MACE

Variables	Univariate HR (95% CI)	P Value	Multivariable HR (95% CI), Manual	P Value	Multivariable HR (95% CI), Automated	P Value
Age	1.05 (1.03–1.07)	<0.001	1.03 (1.0–1.06)	0.04	1.03 (1.0–1.06)	0.04
Sex (male)	1.77 (1.09–2.87)	0.02				
Smoking	0.47 (0.27–0.83)	0.008				
Hypertension	2.29 (1.20–4.35)	0.012				
Diabetes mellitus	1.77 (1.08–2.9)	0.023				
Systolic blood pressure, mm Hg	0.99 (0.98–0.998)	0.016				
Diastolic blood pressure, mm Hg	0.98 (0.96–0.999)	0.034				
Heart rate, beats/min	1.02 (1.01–1.04)	<0.001				
Killip class on admission	2.01 (1.56–2.59)	<0.001	1.43 (1.01–2.02)	0.04	1.51 (1.08–2.12)	0.016
No. of diseased vessels	1.52 (1.14–2.02)	0.004				
Area at risk (%)*	1.01 (1.0–1.03)	0.048				
Manual LVEF† (%)	0.93 (0.91–0.95)	<0.001	0.95 (0.93–0.98)	<0.001		
Automated LVEF† (%)	0.94 (0.92–0.96)	<0.001			0.96 (0.93–0.99)	0.002

HR indicates hazard ratio; LVEF, left ventricular ejection fraction; and MACE, major adverse cardiac events.
*Based on manual late gadolinium enhancement analysis.
†Either manual or automated LVEF was included in multivariable analysis respectively due to high correlation of both parameters.

Table 6.   Univariate and Multivariable Cox Regression Analysis of Patients With Enhancement on LGE Images for Prediction of MACE

Variables	Univariate HR (95% CI)	P Value	Multivariable HR (95% CI), Manual	P Value	Multivariable HR (95% CI), Automated	P Value
Age	1.04 (1.02–1.07)	<0.001	1.03 (1.01–1.06)	0.003	1.03 (1.0–1.06)	0.01
Sex (male)	1.81 (1.09–3.0)	0.02				
Hypertension	2.5 (1.23–5.06)	0.011				
Diabetes mellitus	1.87 (1.11–3.13)	0.018				
Killip class on admission	2.05 (1.58–2.66)	<0.001				
No. of diseased vessels	1.61 (1.19–2.18)	0.002				
Manual IS* (%)	1.04 (1.02–1.06)	<0.001	1.04 (1.02–1.06)	<0.001		
Automated IS* (%)	1.05 (1.02–1.07)	<0.001			1.04 (1.01–1.06)	0.002
Manual MVO (%)	1.09 (1.03–1.15)	0.003				
Automated MVO (%)	1.07 (1.01–1.1)	0.016				
Myocardial salvage index	0.99 (0.98–1.0)	0.048				

HR indicates hazard ratio; IS, infarct size; LGE, late gadolinium enhancement; MACE, major adverse cardiac events. and MVO, microvascular obstruction.
*Either manual or automated IS was included in multivariable analysis, given the high correlation of both parameters.

tomographic angiography, offering improved cardiac risk prediction.[19] Similarly, evidence suggests improved risk prediction in patients with suspected coronary disease using deep learning algorithms for interpreting combined clinical and coronary computed tomographic angiography parameters.[20] Furthermore, recent evidence suggests more individualized and objective likelihood assessment of AMI provided by new AI-derived indexes using the big data approach.[21]

Apart from new classifications and indexes, use of deep learning algorithms optimizes assessment of established parameters that have great impact for current clinical practice. The value of LVEF for risk prediction in patients following AMI is well established.[22–25] Consequently, precise determination of volumetric parameters is important for measuring therapeutic success after coronary reperfusion and clinical decision-making regarding pharmacologic and device therapy.[26,27] In accordance with previous studies, our

automatically generated results revealed better agreement with conventionally generated results for LV assessment than RV analyses.[28] In our work, LV mass and biventricular volumes were principally estimated higher by automated analyses, whereas biventricular ejection fraction was measured lower, which is also consistent with results of other studies based on similar methodology.[5,29] With a mean bias of 2.57% LVEF, which is clinically acceptable, wide CIs ranging from −9.1% to 14.2% underscore the importance of a careful check on results. Even though the method works well in the overall cohort, on an individual basis, experienced observer assessment is necessary to detect outliers for which the analysis has not performed as well. Notwithstanding, LVEF-based risk stratification was similar for manual and automated analyses, suggesting that pathology is adequately captured by both methodologies.

Especially in large patient populations like this cohort, the automated analysis tool reduces required
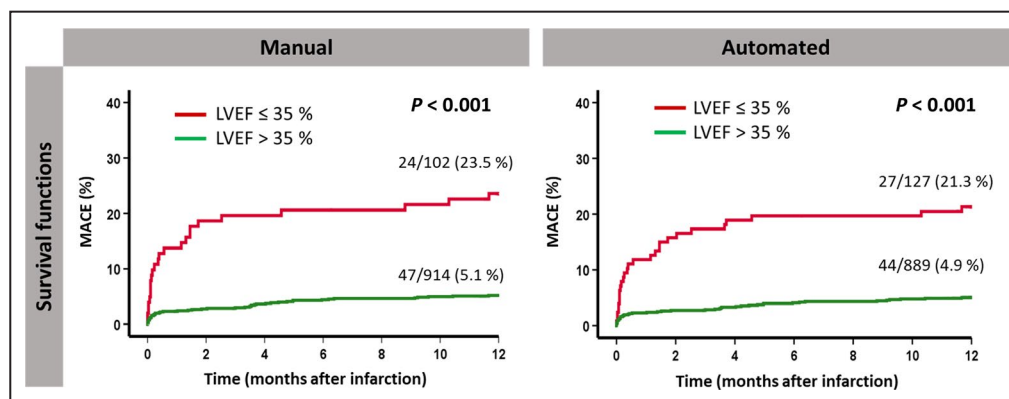
Figure 5.   Kaplan–Meier plots according to LVEF.
Kaplan–Meier curves for manual and automated LVEF analyses presenting the time to MACE in patients dichotomized by clinically relevant LVEF 35% in manual and automated groups, respectively. LVEF indicates left ventricular ejection fraction; and MACE, major adverse cardiac events.

postprocessing time. Compared with standard procedures of manual analyses, the automatic software solution provided ≈10 saved minutes for volumetric assessments and ≈8 minutes for IS quantification per patient, which means a substantial gain of work efficiency.

However, the majority of patients subjectively required manual corrections. Most overall corrections were made in basal slices because their definition is one of the most challenging parts of SAX analyses and is subject to great observer variability.[29] In contrast to our study, some studies have preselected SAX images to simplify the automated analysis at the cost of additional expenditure of time.[30]

In patients with an extended IS resulting in a pronounced LGE, optimal border delineation was aggravated because of a more difficult distinction between hyperintense LGE myocardium and blood pool. Administration of gadolinium contrast agent is known to influence border detection in automated software[30,31]; therefore, it might be taken into consideration by acquiring steady-state free precession–Cine images preferably before giving contrast agent, to lower these effects of a more challenging myocardial border detection using automated software. Regarding time-efficient image acquisition, many CMR scan protocols use the time between giving the contrast agent bolus and LGE scans for steady-state free precession–Cine image acquisition. Nevertheless, even without preselection of images and acquiring the images after gadolinium injection, manual optimization of the automated contours did not lead to better risk prediction or improved diagnostic accuracy based on AUC comparisons; consequently, such optimizations should not be considered mandatory.

It is noteworthy that in contrast to user-independent automatic biventricular volume analyses, automated IS quantification indispensably required manual complementation of potentially present MVO areas within the infarct zone. Therefore, fully automated IS quantification was not yet possible. However, automated "uncorrected" IS including MVO showed similar prognostic implications compared with the manual method. On a different note, this tool enables additional time savings for LGE analyses. It is also conceivable that future software refinements will include deep learning–based detection of MVO.

Taken together, "on-the-fly" postprocessing based on AI seems feasible and could be performed in parallel to other data assessments or during finishing image acquisition.[5] It will be interesting to see whether further refinements of AI algorithms based on continued automated learning may provide further improved risk prediction in large data sets, such as the current AMI patient cohort, in the future.

Study Limitations

CMR imaging in this multicenter study was performed at several different study sites using different CMR vendors. However, all centers followed the same study protocol. Because of contraindications and length of CMR image acquisition, only stable and preselected patients could be included in this study; this approach might result in selection bias, with a lower event rate than in the overall cohort. Nevertheless, this limitation applies to both analysis tools and, consequently, does not limit the validity of the current analysis.

More detailed specifications of the automated algorithm that incorporates AI and deep learning models developed by the manufacturer are not disclosed; therefore, they cannot be described more precisely. Given the missing application of RV mass quantification in the automated algorithm, this parameter was not analyzed.

CONCLUSIONS

User-independent volumetric analyses performed by fully automated software are feasible, and the results are equally predictive of MACE compared with conventional analyses in patients following AMI. Even though a careful check of the results will still be required by an expert physician, this novel technique may provide the tools for time-efficient and reproducible risk stratification in the clinical arena.

Affiliations

From the Department of Cardiology and Pneumology, University Medical Center Göttingen, Georg-August University, Göttingen, Germany (A.S., T.L., S.J.B., C.S., P.C.B., J.M., G.H.); German Centre for Cardiovascular Research (DZHK), partner site Göttingen, Göttingen, Germany (A.S., T.L., S.J.B., C.S., P.C.B., J.M., J.T.K., J.L., M.S., G.H.); Institute for Diagnostic and Interventional Radiology (J.T.K., J.L.) and Department of Pediatric Cardiology (M.S.), University Medical Center Göttingen, Georg-August University, Göttingen, Germany; Helen B. Taussig Heart Center, The Johns Hopkins Hospital and School of Medicine, Baltimore, MD (S.K.); Department of Cardiology, Charité Campus Benjamin Franklin, University Medical Center Berlin, Berlin, Germany (B.B.); Institute of Diagnostic and Interventional Radiology, Heart Center Leipzig at University of Leipzig, Germany (M.G.); Medical Clinic II (Cardiology/Angiology/Intensive Care Medicine), University Heart Center Lübeck, University Hospital Schleswig-Holstein, Lübeck, Germany (S.d.W.-T., T.S., I.E.); German Centre for Cardiovascular Research (DZHK), partner site Hamburg/Kiel/Lübeck, Lübeck, Germany (S.d.W.-T., T.S., I.E.); and Department of Internal Medicine/Cardiology and Leipzig Heart Institute, Heart Center Leipzig at University of Leipzig, Germany (S.D., H.T.).

Disclosures

None.

Supplementary Material

Figure S1

REFERENCES

1. Piepoli MF, Hoes AW, Agewall S, Albus C, Brotons C, Catapano AL, Cooney MT, Corra U, Cosyns B, Deaton C, et al. 2016 European guidelines on cardiovascular disease prevention in clinical practice: the sixth joint Task Force of the European Society of Cardiology and Other Societies on Cardiovascular Disease Prevention in Clinical Practice (constituted by representatives of 10 societies and by invited experts) developed with the special contribution of the European Association for Cardiovascular Prevention & Rehabilitation (EACPR). *Eur Heart J*. 2016;37:2315–2381.

2. Schuster A, Morton G, Chiribiri A, Perera D, Vanoverschelde JL, Nagel E. Imaging in the management of ischemic cardiomyopathy: special focus on magnetic resonance. *J Am Coll Cardiol*. 2012;59:359–370.

3. Bernard O, Lalande A, Zotti C, Cervenansky F, Yang X, Heng PA, Cetin I, Lekadir K, Camara O, Gonzalez Ballester MA, et al. Deep learning techniques for automatic MRI cardiac multi-structures segmentation and diagnosis: is the problem solved? *IEEE Trans Med Imaging*. 2018;37:2514–2525.

4. Bai W, Sinclair M, Tarroni G, Oktay O, Rajchl M, Vaillant G, Lee AM, Aung N, Lukaschuk E, Sanghvi MM, et al. Automated cardiovascular magnetic resonance image analysis with fully convolutional networks. *J Cardiovasc Magn Reson*. 2018;20:65.

5. Backhaus SJ, Staab W, Steinmetz M, Ritter CO, Lotz J, Hasenfuss G, Schuster A, Kowallick JT. Fully automated quantification of biventricular volumes and function in cardiovascular magnetic resonance: applicability to clinical routine settings. *J Cardiovasc Magn Reson*. 2019;21:24.

6. Bhuva AN, Bai W, Lau C, Davies R, Ye Y, Bulluck H, McAlindon E, Culotta V, Swoboda P, Captur G, et al. A multicenter, scan-rescan, human and machine learning cmr study to test generalizability and precision in imaging biomarker analysis. *Circ Cardiovasc Imaging*. 2019;12:e009214.

7. Eitel I, Wohrle J, Suenkel H, Meissner J, Kerber S, Lauer B, Pauschinger M, Birkemeyer R, Axthelm C, Zimmermann R, et al. Intracoronary compared with intravenous bolus abciximab application during primary percutaneous coronary intervention in ST-segment elevation myocardial infarction: cardiac magnetic resonance substudy of the AIDA STEMI trial. *J Am Coll Cardiol*. 2013;61:1447–1454.

8. Eitel I, de Waha S, Wohrle J, Fuernau G, Lurz P, Pauschinger M, Desch S, Schuler G, Thiele H. Comprehensive prognosis assessment by cmr imaging after ST-segment elevation myocardial infarction. *J Am Coll Cardiol*. 2014;64:1217–1226.

9. Schulz-Menger J, Bluemke DA, Bremerich J, Flamm SD, Fogel MA, Friedrich MG, Kim RJ, von Knobelsdorff-Brenkenhoff F, Kramer CM, Pennell DJ, et al. Standardized image interpretation and post processing in cardiovascular magnetic resonance: Society for Cardiovascular Magnetic Resonance (SCMR) board of trustees Task Force on standardized post processing. *J Cardiovasc Magn Reson*. 2013;15:35.

10. Klinke V, Muzzarelli S, Lauriers N, Locca D, Vincenti G, Monney P, Lu C, Nothnagel D, Pilz G, Lombardi M, et al. Quality assessment of cardiovascular magnetic resonance in the setting of the european cmr registry: description and validation of standardized criteria. *J Cardiovasc Magn Reson*. 2013;15:55.

11. Flett AS, Hasleton J, Cook C, Hausenloy D, Quarta G, Ariti C, Muthurangu V, Moon JC. Evaluation of techniques for the quantification of myocardial scar of differing etiology using cardiac magnetic resonance. *JACC Cardiovasc Imaging*. 2011;4:150–156.

12. Bland JM, Altman DG. Statistical methods for assessing agreement between two methods of clinical measurement. *Lancet*. 1986;1:307–310.

13. Kowallick JT, Morton G, Lamata P, Jogiya R, Kutty S, Lotz J, Hasenfuss G, Nagel E, Chiribiri A, Schuster A. Inter-study reproducibility of left ventricular torsion and torsion rate quantification using mr myocardial feature tracking. *J Magn Reson Imaging*. 2016;43:128–137.

14. Gertz RJ, Lange T, Kowallick JT, Backhaus SJ, Steinmetz M, Staab W, Kutty S, Hasenfuss G, Lotz J, Schuster A. Inter-vendor reproducibility of left and right ventricular cardiovascular magnetic resonance myocardial feature-tracking. *PLoS One*. 2018;13:e0193746.

15. Grothues F, Smith GC, Moon JC, Bellenger NG, Collins P, Klein HU, Pennell DJ. Comparison of interstudy reproducibility of cardiovascular magnetic resonance with two-dimensional echocardiography in normal subjects and in patients with heart failure or left ventricular hypertrophy. *Am J Cardiol*. 2002;90:29–34.

16. DeLong ER, DeLong DM, Clarke-Pearson DL. Comparing the areas under two or more correlated receiver operating characteristic curves: a nonparametric approach. *Biometrics*. 1988;44:837–845.

17. Krittanawong C, Zhang H, Wang Z, Aydar M, Kitai T. Artificial intelligence in precision cardiovascular medicine. *J Am Coll Cardiol*. 2017;69:2657–2664.

18. Betancur J, Commandeur F, Motlagh M, Sharir T, Einstein AJ, Bokhari S, Fish MB, Ruddy TD, Kaufmann P, Sinusas AJ, et al. Deep learning for prediction of obstructive disease from fast myocardial perfusion SPECT: a multicenter study. *JACC Cardiovasc Imaging*. 2018;11:1654–1663.

19. Oikonomou EK, Williams MC, Kotanidis CP, Desai MY, Marwan M, Antonopoulos AS, Thomas KE, Thomas S, Akoumianakis I, Fan LM, et al. A novel machine learning-derived radiotranscriptomic signature of perivascular fat improves cardiac risk prediction using coronary ct angiography. *Eur Heart J*. 2019;40:3529–3543.

20. Motwani M, Dey D, Berman DS, Germano G, Achenbach S, Al-Mallah MH, Andreini D, Budoff MJ, Cademartiri F, Callister TQ, et al. Machine learning for prediction of all-cause mortality in patients with suspected coronary artery disease: a 5-year multicentre prospective registry analysis. *Eur Heart J*. 2017;38:500–507.

21. Than MP, Pickering JW, Sandoval Y, Shah ASV, Tsanas A, Apple FS, Blankenberg S, Cullen L, Mueller C, Neumann JT, et al. Machine learning to predict the likelihood of acute myocardial infarction. *Circulation*. 2019;140:899–909.

22. Pelliccia F, Pasceri V, Niccoli G, Tanzilli G, Speciale G, Gaudio C, Crea F, Camici PG. Predictors of long-term mortality in patients with myocardial infarction and nonobstructed coronary arteries: a systematic review and meta-regression study. *Am J Med*. 2020;133:73–83.e4.

23. White HD, Norris RM, Brown MA, Brandt PW, Whitlock RM, Wild CJ. Left ventricular end-systolic volume as the major determinant of survival after recovery from myocardial infarction. *Circulation*. 1987;76:44–51.

24. McClements BM, Weyman AE, Newell JB, Picard MH. Echocardiographic determinants of left ventricular ejection fraction after acute myocardial infarction. *Am Heart J*. 2000;140:284–289.

25. Eitel I, Stiermaier T, Lange T, Rommel KP, Koschalka A, Kowallick JT, Lotz J, Kutty S, Gutberlet M, Hasenfuss G, et al. Cardiac magnetic resonance myocardial feature tracking for optimized prediction of cardiovascular events following myocardial infarction. *JACC Cardiovasc Imaging*. 2018;11:1433–1444.

26. Ibanez B, James S, Agewall S, Antunes MJ, Bucciarelli-Ducci C, Bueno H, Caforio ALP, Crea F, Goudevenos JA, Halvorsen S, et al. 2017 ESC guidelines for the management of acute myocardial infarction in patients presenting with st-segment elevation: the Task Force for the management of acute myocardial infarction in patients presenting with ST-segment elevation of the European Society of Cardiology (ESC). *Eur Heart J*. 2018;39:119–177.

27. Roffi M, Patrono C, Collet JP, Mueller C, Valgimigli M, Andreotti F, Bax JJ, Borger MA, Brotons C, Chew DP, et al. 2015 ESC guidelines for the management of acute coronary syndromes in patients presenting without persistent ST-segment elevation: Task Force for the management of acute coronary syndromes in patients presenting without persistent ST-segment elevation of the European Society of Cardiology (ESC). *Eur Heart J*. 2016;37:267–315.

28. Hudsmith LE, Petersen SE, Francis JM, Robson MD, Neubauer S. Normal human left and right ventricular and left atrial dimensions using steady state free precession magnetic resonance imaging. *J Cardiovasc Magn Reson*. 2005;7:775–782.

29. Bhuva AN, Treibel TA, De Marvao A, Biffi C, Dawes TJW, Doumou G, Bai W, Patel K, Boubertakh R, Rueckert D, et al. Sex and regional differences in myocardial plasticity in aortic stenosis are revealed by 3D model machine learning. *Eur Heart J Cardiovasc Imaging*. 2020;21:417–427.

30. Fathi A, Weir-McCall JR, Struthers AD, Lipworth BJ, Houston G. Effects of contrast administration on cardiac MRI volumetric, flow and pulse wave velocity quantification using manual and software-based analysis. *Br J Radiol*. 2018;91:20170717.

31. Moccia S, Banali R, Martini C, Muscogiuri G, Pontone G, Pepi M, Caiani EG. Development and testing of a deep learning-based strategy for scar segmentation on CMR-LGE images. *MAGMA*. 2019;32:187–195.